Analytical approach to phonons and electron–phonon interactions in single-walled zigzag carbon nanotubes

2008 J. Phys.: Condens. Matter 20 325222

(http://iopscience.iop.org/0953-8984/20/32/325222)

IOP PUBLISHING JOURNAL OF PHYSICS: CONDENSED MATTER

J. Phys.: Condens. Matter **20** (2008) 325222 (7pp) doi:10.1088/0953-8984/20/32/325222

Analytical approach to phonons and electron–phonon interactions in single-walled zigzag carbon nanotubes

B S Kandemir and M Keskin

Department of Physics, Faculty of Sciences, Ankara University, 06100 Tandoğan, Ankara, Turkey

Received 11 April 2008, in final form 24 June 2008
Published 18 July 2008
Online at stacks.iop.org/JPhysCM/20/325222

Abstract

In this paper, exact analytical expressions for the entire phonon spectra in single-walled carbon nanotubes with zigzag geometry are presented by using a new approach, originally developed by Kandemir and Altanhan. This approach is based on the concept of construction of a classical lattice Hamiltonian of single-walled carbon nanotubes, wherein the nearest and next nearest neighbor and bond bending interactions are all included, then its quantization and finally diagonalization of the resulting second quantized Hamiltonian. Furthermore, within this context, explicit analytical expressions for the relevant electron–phonon interaction coefficients are also investigated for single-walled carbon nanotubes having this geometry, by the phonon modulation of the hopping interaction.

In a previous paper [1] (henceforth referred to as I), we propose a self-consistent analytical procedure that allows us to calculate the phonon dispersion relations in single-walled carbon nanotubes (SWCNTs). Qualitatively, it consists of three main stages: first, we construct, from the geometrical considerations, a classical Hamiltonian for lattice vibrations in SWCNTs by taking into account only the nearest and next nearest neighbor as well as bond bending interactions, in terms of generalized coordinates; second, a diagonalization procedure through two subsequent unitary transformations for the quantized Hamiltonian, i.e. for the phonon Hamiltonian, is performed; finally, we investigate the exact analytical expressions for the electron–phonon interaction amplitudes in these structures. Furthermore, we introduce a diagonalization procedure for the tight-binding electronic Hamiltonian so as to be consistent with the diagonalization scheme performed in the phonon part. Subsequently, we derive the analytical dispersion relations for whole phonon modes in SWCNTs, along with the description of analytical electron–phonon interaction terms corresponding to these modes, within the Fröhlich sense. However, to be self-contained, there we limit ourselves to the discussion of phonon spectra in SWCNTs with armchair geometry only. In the present paper, both analytical phonon dispersion relations and associated electron–phonon interaction amplitudes in single-walled zigzag carbon nanotubes will be investigated.

Historically, since the discovery of carbon nanotubes [2] and their subsequent syntheses [3, 4], there exist various experimental and theoretical investigations on the physical properties of these novel materials [5–9]. In particular, the observation of superconductivity in nanotubes [10] and nanotube ropes [11], electron–phonon interactions and superconductivity [12] have been a focus of interest in these one-dimensional systems. In the literature, within only the last few years, there has been a dramatic growth of interest in studies on phonon dispersion relations in SWCNTs [13–23]. Moreover, due to their crucial role in understanding electronic, optical and transport properties of these structures, many theoretical investigations in electron–phonon interactions have also been performed. Of these, so far, electron–phonon interaction studies in nanotubes are achieved by employing the tight-binding model, for the interaction of electrons with acoustical phonons [24] and for linear electron–phonon coupling displaying a deformation type of approximation [25]. Scattering by optical phonons is also important for transport properties and for the major source of broadening for certain Raman peaks [26]. The first attempt to calculate the interaction of an electron with acoustical and optical phonons is achieved by assuming phonon modulation of the hopping interaction in armchair and zigzag nanotubes [27]. Recently, the electron–phonon matrix element in SWCNTs is developed by density functional theory [28] within the tight-binding approach. The effect of electron–phonon interaction on

the Raman intensity [29], and intraband scattering [30], is considered within a symmetry-adapted nonorthogonal tight-binding model. A study of lattice vibrations in SWCNTs based on a force-constant model is also notable [31].

In this paper, we investigate analytical phonon frequencies for zigzag SWCNTs together with associated electron–phonon interactions, based on the same arguments in our earlier work. Since, except for geometrical differences, analytical considerations of zigzag SWCNTs will be similar to those of armchair SWCNTs as outlined in I, the same arguments can then be directly extended to the case of the phonon dispersion curves of $(n, 0)$ SWCNTs. To achieve this, we shall briefly review our model, by recalling the main features of the scheme proposed in I needed to extend it to zigzag SWCNTs. In particular, we believe that emphasizing the differences arising from the geometry will be explanatory itself, so as to provide a recipe for how the considerations of these two subsequent publications can be extended to more complicated structures, or at least provide an algorithm for future numerical studies in such structures.

On the basis of the procedure described in I, by dropping the off-diagonal terms, the total Hamiltonian of a system of electrons and phonons in SWCNTs is found to be composed of two terms as follows:

$$H = \sum_{\mathbf{k}} \left[E^{(+)} C^{\dagger}_{\mathrm{A},\mathbf{k}} C_{\mathrm{A},\mathbf{k}} + E^{(-)} C^{\dagger}_{\mathrm{B},\mathbf{k}} C_{\mathrm{B},\mathbf{k}} \right] + \sum_{i} H_i \quad (1)$$

with

$$H_i = \sum_{\mathbf{q}} \hbar\widetilde{\omega}_i(\mathbf{q}) \left(a^{\dagger}_{\mathbf{q}i} a_{\mathbf{q}i} + \tfrac{1}{2} \right) + \sum_{\mathbf{q}} \sum_{\mathbf{k}} \mathcal{D}_i(\mathbf{k}, \mathbf{q}) \times \left(a^{\dagger}_{\mathbf{q}i} + a_{\mathbf{q}i} \right). \quad (2)$$

Here, the first term in equation (1) is, after a proper Bogoliubov unitary transformation proposed first in I, the well known spinless tight-binding Hamiltonian with energies $E^{(\pm)} = \pm J_0 |\Theta(\mathbf{k})|$, where J_0 is the hopping parameter and takes a value of approximately 2.4–3.1 eV, and $\Theta(\mathbf{k})$ is the sum of phase factors of atom A with its three nearest neighbor B atoms or vice versa. $C^{\dagger}_{\mathrm{A(B)},\mathbf{k}}$ and $C_{\mathrm{A(B)},\mathbf{k}}$ are the creation and annihilation operators for an electron with mode $\mathbf{k}$, respectively. In equations (1) and (2) i is the phonon band index and runs from 1 to 6. The second term in equation (1) is portioned again into the sum of two terms, as in equation (2): while the former is the Hamiltonian of the free phonon field, the latter accounts for the electron–phonon interaction Hamiltonian, and is represented with the interaction amplitude given by

$$\mathcal{D}_i(\mathbf{k}, \mathbf{q}) = \left[\mathcal{L}^{(-)}_i C^{\dagger}_{\mathrm{B},\mathbf{k}+\mathbf{q}} C_{\mathrm{B},\mathbf{k}} - \mathcal{L}^{(+)}_i C^{\dagger}_{\mathrm{A},\mathbf{k}+\mathbf{q}} C_{\mathrm{A},\mathbf{k}} \right] + \exp(+\mathrm{i}\xi) \left[\mathcal{L}^{(+)}_i C^{\dagger}_{\mathrm{A},\mathbf{k}+\mathbf{q}} C_{\mathrm{B},\mathbf{k}} + \exp(-\mathrm{i}\xi)\, \mathcal{L}^{(-)}_i C^{\dagger}_{\mathrm{B},\mathbf{k}+\mathbf{q}} C_{\mathrm{A},\mathbf{k}} \right] \quad (3)$$

with $\Psi_{\pm} = \{\exp[-\mathrm{i}\xi(\mathbf{k})] \pm \exp[+\mathrm{i}\xi(\mathbf{k}+\mathbf{q})]\}/2$ and $\mathcal{L}^{(\pm)}_i = \mathcal{M}^{\mathrm{T}(+)}_i \Psi^{*}_{+} \pm \mathcal{M}^{\mathrm{T}(-)}_i \Psi^{*}_{-}$. In equation (2), $a^{\dagger}_{\mathbf{q}i}$ and $a_{\mathbf{q}i}$ are the creation and annihilation operators for phonons, respectively for $\mathbf{q}$ modes. ξ is the argument of the $\Theta(\mathbf{k})$ and $\mathcal{M}^{\mathrm{T}(\pm)}_i$ is

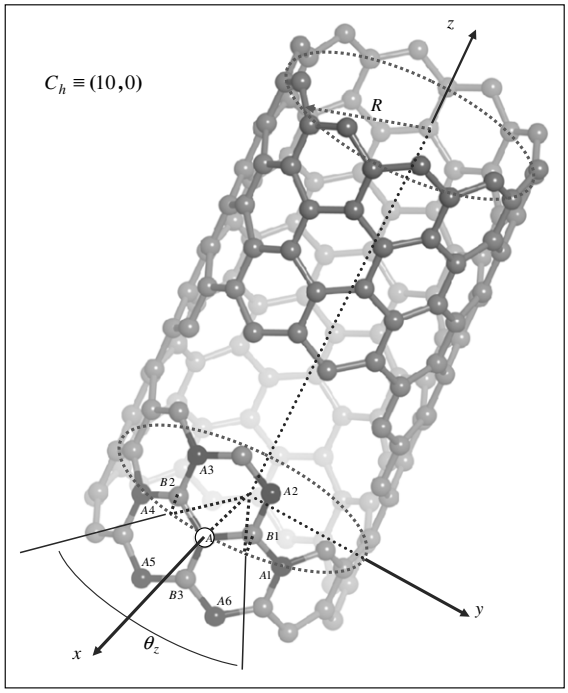

Figure 1. A three-dimensional plot of a (10, 0) zigzag SWCNT showing the nearest and next nearest neighbors of carbon atom A.

the electron–phonon interaction amplitudes for intraband and interband scattering whose exact analytical expressions are all obtained in the framework of the theory developed here. In other words, while the first term in equation (3) represents the intraband scattering of an electron from the carbon atom A (B) with wavevector $\mathbf{k} \equiv (k, \gamma)$ to the state with wavevector $\mathbf{q} + \mathbf{k} \equiv (q + k, \alpha + \gamma)$ of the carbon atom A (B), the second one describes the interband scattering of an electron from the carbon atom A (B) with wavevector $\mathbf{k} \equiv (k, \gamma)$ to the state with wavevector $\mathbf{q} + \mathbf{k} \equiv (q + k, \alpha + \gamma)$ of the carbon atom B (A).

Here, it should be stated that, for the most part, geometric considerations, i.e. the notation used in construction of a zigzag SWCNT, are due to Jeon and Mahan [22]. The key difference between armchair and zigzag SWCNTs is simply that their geometric structures are different. In contrast to armchair filling, for zigzag geometry we again consider two types of carbon atom A and B in a unit cell but require, as shown in figure 1, the two-dimensional graphene plane to be filled by hexagons so as to give a zigzag geometry when rolled up around the z axis [32, 33]. In order to define the coordinates of the zigzag SWCNT to be used as the basis for our formulation, we first define the angle θ_z between A and B atoms along the circumference. From the geometric construction, it can be easily shown that the relation $\sin(\theta_z/2) = a\sqrt{3}/2R$ holds and it reduces to $\theta_z \approx a\sqrt{3}/R$ for zigzag SWCNTs with large radius.

By constructing the zigzag SWCNT, we consider a hexagonal lattice of carbon atoms as presented in I, but we draw it here vertically as in figure 2. The lattice coordinates of this structure are still defined by the vectors $\mathbf{R}_{ij} = i\mathbf{a}_1 + j\mathbf{a}_2$ with integer i and j, but now where $\mathbf{a}_1 = \sqrt{3}a(1, \sqrt{3})/2$

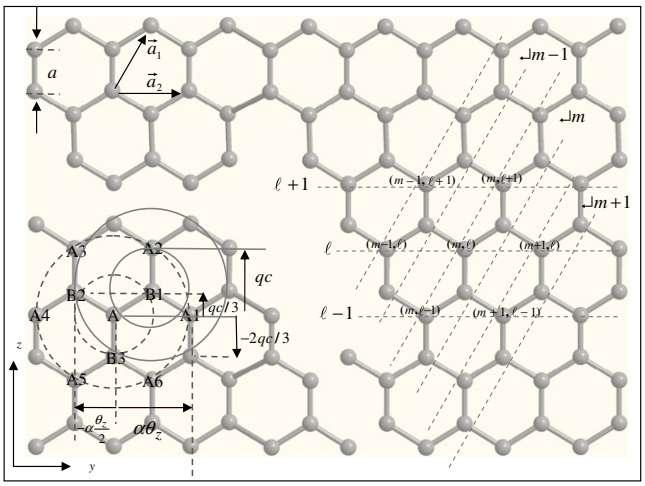

Figure 2. Graphene. Rolling it up around the z-axis results in an SWCNT having zigzag geometry, as shown in figure 1. Graphical illustrations of nearest and next nearest neighbors of A (B1) atoms are also given in the same picture together with the relevant phases.

and $\mathbf{a}_2 = \sqrt{3}a(1, 0)$ are the base vectors, as shown in (x, y) coordinate systems in figure 2, whose magnitude is the lattice constant of graphene, i.e. $\sqrt{3}a$, where a is the nearest neighbor distance between two carbon atoms, i.e., $a = a_{\mathrm{C–C}} = 1.42$ Å. When this plane is rolled up into a cylinder to form a zigzag tube $(n, 0)$, the coordinates are to be designated by $\mathbf{R}_{\ell m} = \ell\mathbf{a}_1 + m(\mathbf{a}_1 + \mathbf{a}_2)$, where the integer ℓ denotes the position along the z-axis and takes the values of $\ell = 0, 1, \ldots, N$. Here, N is the number of atomic layers along the z-axis, and m labels the carbon atoms along the circumference of the tube and takes the values of $m = 0, 1, \ldots, n-1$. [27, 34, 35]

Accordingly, it is easy to show that the lattice coordinates of this two-dimensional graphene plane are now defined by the vectors

$$\mathbf{R}_{\mathrm{A},m\ell} = [R\cos(\theta_{m\ell}), R\sin(\theta_{m\ell}), c\ell], \tag{4}$$

three nearest neighbor B type atoms at

$$\mathbf{R}_{\mathrm{B},m\ell} = \left[R\cos\left(\theta_{m\ell} + \frac{\theta_z}{2}\right), R\sin\left(\theta_{m\ell} + \frac{\theta_z}{2}\right), c\ell + \frac{a}{2}\right],$$
$$\mathbf{R}_{\mathrm{B},m-1,\ell} = \left[R\cos\left(\theta_{m\ell} - \frac{\theta_z}{2}\right), R\sin\left(\theta_{m\ell} - \frac{\theta_z}{2}\right), c\ell + \frac{a}{2}\right],$$
$$\mathbf{R}_{\mathrm{B},m,\ell-1} = [R\cos(\theta_{m\ell}), R\sin(\theta_{m\ell}), c\ell - a], \tag{5}$$

and six next nearest neighbor A type atoms at

$$\mathbf{R}_{\mathrm{A},m,\ell\mp1} = \left[R\cos\left(\theta_{m\ell} \mp \frac{\theta_z}{2}\right), R\sin\left(\theta_{m\ell} \mp \frac{\theta_z}{2}\right), c(\ell \mp 1)\right],$$
$$\mathbf{R}_{\mathrm{A},m\pm1,\ell\mp1} = \left[R\cos\left(\theta_{m\ell} \pm \frac{\theta_z}{2}\right), R\sin\left(\theta_{m\ell} \pm \frac{\theta_z}{2}\right), c(\ell \mp 1)\right], \tag{6}$$
$$\mathbf{R}_{\mathrm{A},m\pm1,\ell} = \left[R\cos(\theta_{m\ell} \pm \theta_z), R\sin(\theta_{m\ell} \pm \theta_z), c\ell\right],$$

where $\theta_z = 2\pi/n$ and $c = 3a/2$. In fact, $\theta_{m\ell}$ is the angle seen by two adjacent A or two adjacent B carbon atoms along the circumference of the tube. First, by using equations (5)and (6) together with equation (4) one can readily introduce three unit vectors connecting atom A to its three nearest neighbor B atoms, then six unit vectors between atom A and its six next nearest neighbor A atoms. Second, to construct the potential part of the phonon Hamiltonian, these unit vectors are used to get the nearest and next nearest neighbor interactions, given by terms proportional to squares of $\chi^{(i)k}_{\mathbf{q},j} = \delta^k_i \cdot (\mathbf{Q}^{(i)}_k - \mathbf{Q}_{\mathrm{A}})$, where $k = 1$ for nearest and $k = 2$ for next nearest neighbor displacements. Finally, considering bond bending interactions of the form $\Delta_{\mathrm{B(A)}} = \sum_{i=1}^{3} \mathbf{n}_i \cdot [\mathbf{Q}^{(i)}_{\mathrm{A(B)}} - \mathbf{Q}^{(0)}_{\mathrm{B(A)}}]$ completes the scheme.

To be able to write the classical Hamiltonian representing the lattice vibrations, which is first proposed in I, and thereby to make the transition to its quantized version, we first introduce matrix notation for the lattice displacements, such as a 6×1 column vector $\mathbb{Q}$, with Hermitian conjugate $\mathbb{Q}^\dagger = (\,Q^*_{\mathrm{A}\rho} \;\; Q^*_{\mathrm{A}\theta} \;\; Q^*_{\mathrm{A}z} \;\; Q^*_{\mathrm{B}\rho} \;\; Q^*_{\mathrm{B}\theta} \;\; Q^*_{\mathrm{B}z}\,)$. Then, the total Hamiltonian for the SWCNTs can be arranged into the form

$$H_{\mathrm{lat}} = \tfrac{1}{2}M \sum_{\mathbf{q}\equiv(q,\alpha)} \dot{\overline{\mathbb{Q}}}^\dagger \, \mathbb{C}^\dagger \, \mathbb{C}\dot{\overline{\mathbb{Q}}} + \tfrac{1}{2}K_1 \sum_{\mathbf{q}\equiv(q,\alpha)} \overline{\mathbb{Q}}^\dagger \, \mathbb{D} \, \overline{\mathbb{Q}}, \tag{7}$$

where $\mathbb{D} = \mathbb{C}^\dagger\overline{\mathbb{A}}\mathbb{C} = \sum_{k=1}^{3} r_k \mathbb{C}^\dagger \mathbb{A}^k \mathbb{C}$ has been used with $\overline{\mathbb{A}}_{ij} = \sum_{k=1}^{3} r_k \, \mathbb{A}^k_{ij}$. The elements of the matrix $\mathbb{D}$ in equation (7) are defined as $\mathbb{D}_{ij} = \widetilde{\mathbb{A}}_{ij}$ for i (j) $= 1, 2, 3$ $(1, 2, 3)$; $\mathbb{D}_{ij} = \widetilde{\mathbb{A}}_{ij}/2$ for i (j) $= 1, 2, 3$ $(4, 5, 6)$ and j (i) $= 4, 5, 6$ $(1, 2, 3)$; $\mathbb{D}_{ij} = \widetilde{\mathbb{A}}_{ij}/4$ for i (j) $= 4, 5, 6$ $(4, 5, 6)$. From the above zigzag geometry considerations, the diagonal elements of $\widetilde{\mathbb{A}}_{ij}$ can easily be found in terms of $\overline{\mathbb{A}}_{ij}$, whose non-zero elements are all presented in the appendix,

$$\begin{aligned}
\widetilde{\mathbb{A}}_{11} &= \left[3\,(s_z)^2\, C_1^{(+)}\right] + 8\widetilde{r}_2\left[2\,(\widetilde{s}_z)^2\,(\widetilde{c}_\alpha)^2 + (s_z)^2\, S_2^{(0)}\right] \\
&\quad + 4\widetilde{r}_3 C_3^{(-)} \\
\widetilde{\mathbb{A}}_{22} &= \left[3c_z^2 C_1^{(-)}\right] + 8\widetilde{r}_2\left[2\,(\widetilde{c}_z)^2\,(\widetilde{s}_\alpha)^2 + (c_z)^2\, C_2^{(0)}\right] \\
&\quad + 8\widetilde{r}_3\,(s_z)^2\,\widetilde{s}_\alpha^2 \\
\widetilde{\mathbb{A}}_{33} &= \left[3 - C_1^{(0)}\right] + 24\widetilde{r}_2 C_2^{(0)} \\
\widetilde{\mathbb{A}}_{44} &= \left[3\,(s_z)^2\, C_1^{(-)}\right] + 8\widetilde{r}_2\left[2\,(\widetilde{s}_z)^2\,(\widetilde{c}_\alpha)^2 + (s_z)^2\, S_2^{(0)}\right] \\
&\quad + 4\widetilde{r}_3 C_3^{(+)} \\
\widetilde{\mathbb{A}}_{55} &= \left[3c_z^2 C_1^{(+)}\right] + 8\widetilde{r}_2\left[2\,(\widetilde{c}_z)^2\,(\widetilde{s}_\alpha)^2 + (c_z)^2\, C_2^{(0)}\right] \\
&\quad + 8\widetilde{r}_3\,(s_z)^2\,\widetilde{s}_\alpha^2 \\
\widetilde{\mathbb{A}}_{66} &= \left[3 + C_1^{(0)}\right] + 24\widetilde{r}_2 C_2^{(0)}
\end{aligned} \tag{8}$$

with

$$C_1^{(\pm)} = 1 \pm c_{3q}\widetilde{c}_\alpha$$
$$C_1^{(0)} = c_{3q}\widetilde{c}_\alpha + 2\left(2c_{3q}^2 - 1\right)$$

$$C_2^{(0)} = 1 + 2c_{2q}^2 s_\alpha^2 - c_{2q}^2 - s_\alpha^2$$
$$S_2^{(0)} = 1 + 2s_{2q}^2 s_\alpha^2 - s_{2q}^2 - s_\alpha^2$$
$$C_3^{(\pm)} = 1 + 2c_z\left(1 + \widetilde{c}_\alpha c_{1q}\right) + 2c_z^2\left(1 + \widetilde{c}_\alpha^2\right) \pm (1 + 2c_z)\left(2c_{3q}^2 - 1 + 2\widetilde{c}_\alpha c_z c_{3q}\right),$$

while the non-diagonal and non-zero terms are given by

$$\left.\begin{matrix}\mathrm{Re}\widetilde{\mathbb{A}}_{24}\\ \mathrm{Re}\widetilde{\mathbb{A}}_{15}\end{matrix}\right\} = \mp 3 s_z c_z s_{3q}\widetilde{s}_\alpha \mp 4\widetilde{r}_3 s_z \widetilde{s}_\alpha \left[s_{3q}\left(1 + 2c_z\right) \pm s_{1q}\right]$$
$$\left.\begin{matrix}\mathrm{Re}\widetilde{\mathbb{A}}_{16}\\ \mathrm{Re}\widetilde{\mathbb{A}}_{34}\end{matrix}\right\} = -\sqrt{3}s_z\left(1 \pm c_{3q}\widetilde{c}_\alpha\right) \qquad (9)$$
$$\left.\begin{matrix}\mathrm{Re}\widetilde{\mathbb{A}}_{23}\\ \mathrm{Re}\widetilde{\mathbb{A}}_{56}\end{matrix}\right\} = \pm\sqrt{3}c_z s_{3q}\widetilde{s}_\alpha + 4\sqrt{3}\widetilde{r}_3 c_z \widetilde{s}_\alpha s_{1q},$$

respectively, where we have used the following abbreviations: $\widetilde{s}_\alpha = \sin(\alpha\theta_z/2)$, $\widetilde{c}_\alpha = \cos(\alpha\theta_z/2)$, $s_\alpha = \sin(\alpha\theta_z/4)$, $c_\alpha = \cos(\alpha\theta_z/4)$, $s_{nq} = \sin(qc/n)$ and $c_{nq} = \cos(qc/n)$.

Now, we introduce $a_{\mathbf{q}\beta}^\dagger$ and operators $a_{\mathbf{q}\beta}$ for the lattice displacements, where $a_{\mathbf{q}\beta}$ ($a_{\mathbf{q}\beta}^\dagger$) defines annihilation (creation) operators for the center of mass and relative motions $\beta = 1, 2, 3$, and $\beta = 4, 5, 6$, separately, and then we rearrange equation (7) into the second quantized form. Finally, after the first unitary transformation, $U_1 = \exp[S_1(\mathbf{q})]$ with $S_1(\mathbf{q}) = \sum_k \lambda_k(a_{\mathbf{q}k}^2 - a_{\mathbf{q}k}^{\dagger 2})/2$, which in fact partially diagonalizes the quantized lattice Hamiltonian, it is easily verified that it becomes

$$\overline{\widetilde{H}}_{\mathrm{ph}} = \frac{1}{2}\sum_{\mathbf{q}}\sum_{i=1}^{6}\left[\hbar\overline{\omega}_i^{(0)}(\mathbf{q})\left(a_{\mathbf{q}i}^\dagger a_{\mathbf{q}i} + a_{\mathbf{q}i}a_{\mathbf{q}i}^\dagger\right) + \sum_{j(\neq i)}\hbar\overline{\omega}_{ij}^{(0)}(\mathbf{q})\left(a_{\mathbf{q}i}^\dagger a_{\mathbf{q}j} + a_{\mathbf{q}i}^\dagger a_{\mathbf{q}j}^\dagger + \mathrm{H.c.}\right)\right], \qquad (10)$$

with $\overline{\omega}_i^{(0)}(\mathbf{q}) = (\widetilde{\mathbb{A}}_{ii}/6)^{1/2}$, $\overline{\omega}_{ij}^{(0)}(\mathbf{q}) = \mathrm{Re}\,\widetilde{\mathbb{A}}_{ij}/2\sqrt{6}(\widetilde{\mathbb{A}}_{ii}\widetilde{\mathbb{A}}_{jj})^{1/4}$. It should be noticed that first, a rescaling of phonon frequencies and therefore phonon energy to the well known Raman line, $\omega_0 = 1600\ \mathrm{cm}^{-1}$, which is defined by the relation $K_1/M = \omega_0^2/3$, has been performed for the sake of making the total Hamiltonian in dimensionless form. In other words, hereafter, dimensionless energy and frequencies will be used as $\overline{H} = \widetilde{H}/\hbar\omega_0$, $\overline{\omega}_i^{(0)}(\mathbf{q}) = \omega_i^{(0)}(\mathbf{q})/\omega_0$, $\overline{\omega}_{ij}^{(0)}(\mathbf{q}) = \omega_{ij}^{(0)}(\mathbf{q})/\omega_0$. In our theoretical treatment we have used two adjustable parameters, the ratios of spring constants $\widetilde{r}_2 = K_2/K_1$ and $\widetilde{r}_3 = K_3/K_1$. We take these two scaling factors for force-constant parameters[1] as $\widetilde{r}_2 = 0.060, \widetilde{r}_3 = 0.024$ as in [22]. This diagonalization does not give satisfactory results for the phonon spectra (see the left panel of figure 3), therefore further diagonalization of the nonlinear terms in equation (10) is needed. Therefore, we introduce the second unitary transformation, $U_2 = \exp[S_2(\mathbf{q})]$ with $S_2(\mathbf{q}) = \sum_{j\neq i}\lambda_j(a_{\mathbf{q}i}a_{\mathbf{q}j}^\dagger - a_{\mathbf{q}i}^\dagger a_{\mathbf{q}j})$. The entire procedure of such a diagonalization of equation (10) is documented in I in detail and therefore will not be repeated here. After

[1] It should be noted here that, to make a comparison with those calculated in [22], we have taken two scaling factors to be $\widetilde{r}_2 = 0.060$, $\widetilde{r}_3 = 0.024$, in contrast to those indicated in their work. In fact, though in [22] they have indicated a different set of parameters, i.e. $\widetilde{r}_2 = 0.090, \widetilde{r}_3 = 0.033$, they have used our parameters in performing their numerical calculations. Nevertheless, the same calculations can also be easily done with this set.

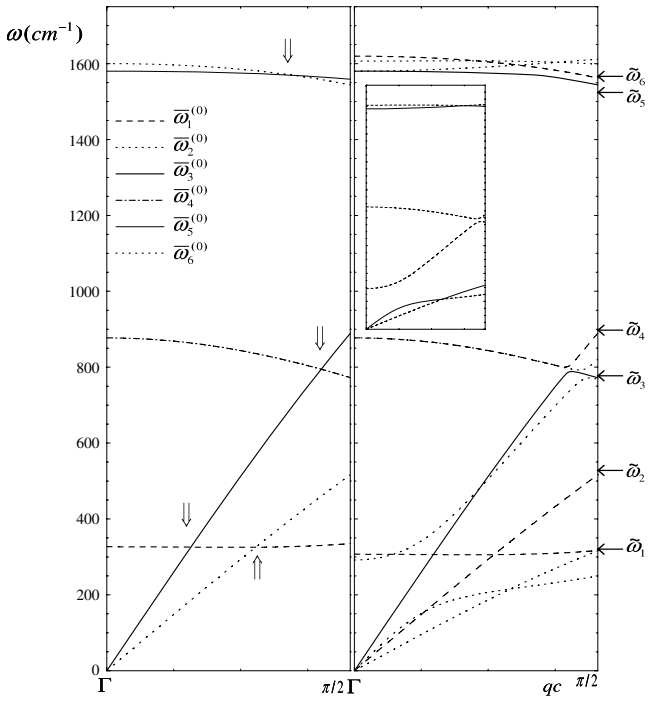

Figure 3. For a (10, 0) zigzag SWCNT with $\alpha = 0$, q-dependence of the phonon spectra according to $\overline{\omega}_i^{(0)}$ (left panel), arising from the first diagonalization. In the right panel, again q-dependence of the phonon spectra, but after the second unitary transformation, according to equation (12), together with their comparison with those found by Jeon and Mahan (the solid and dashed lines correspond to the results of equation (12), the dotted lines to those of [21]). To make the comparison easy, the results of [21] are also given in the inset.

the unitary transformation, by dropping the higher order terms, equation (10) can be rearranged into the form

$$H_{i,\mathrm{ph}} = \tfrac{1}{2}\sum_{\mathbf{q}\equiv(q,\alpha)}\widetilde{\omega}_i\left(a_{\mathbf{q}i}^\dagger a_{\mathbf{q}i} + a_{\mathbf{q}i}a_{\mathbf{q}i}^\dagger\right), \qquad (11)$$

with

$$\widetilde{\omega}_i(\mathbf{q}) = \tfrac{1}{3}\left[-\widetilde{\Omega}_{(ijk)}^{(2)} + 2\widetilde{\Omega}_{(ijk)}^{(+)}\cos\tfrac{1}{3}\widetilde{\Omega}_{(ijk)}\right] \qquad (12)$$

where $\widetilde{\omega}_i$ are the solutions of a cubic algebraic equation. Here, $\widetilde{\Omega}_{(ijk)}^{(2)}$, $\widetilde{\Omega}_{(ijk)}^{(+)}$ and $\widetilde{\Omega}_{(ijk)}$ are functions of $\widetilde{\mathbb{A}}_{ij}$ given by equations (8) and (9).

Further, we shall consider the electron–phonon interactions in zigzag SWCNTs. The knowledge of phonon frequencies in these structures allows us directly to calculate electron–phonon interaction amplitudes analytically. The treatment of electron–phonon interaction amplitude is one of the central issues of our previous work and will not be repeated here. But, to summarize, our calculations proceed in three stages: first, we calculate the effect of two successive transformations for the phonon part on this interaction; then, we take into account the effect of the unitary transformation for the electronic part of the electron–phonon interaction amplitude; then, we get the interaction amplitudes from the resulting Hamiltonian. This procedure results in the second part of equation (2), with the co-

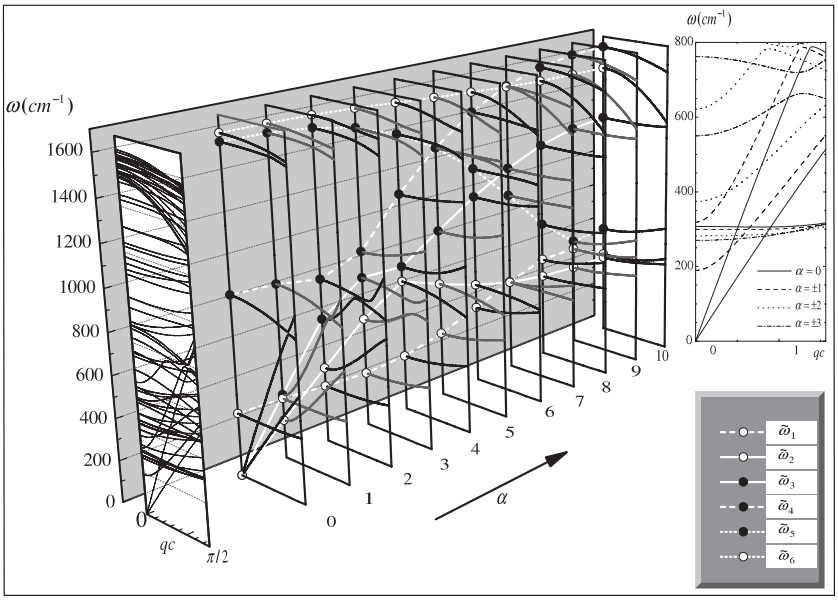

Figure 4. Plot of $\widetilde{\omega}_i(\mathbf{q})$ according to equation (12) from $\alpha = 0$ to 10 for a $(10, 0)$ zigzag SWCNT. The inset shows the low frequency–small wavevector region.

efficients of $\mathcal{M}_i^{\mathrm{T}(\pm)}(\mathbf{q}, \mathbf{k}) = \cos\Lambda\overline{\mathbb{M}}_i^{\mathrm{T}(\pm)}(\mathbf{q}, \mathbf{k})$ given in equation (3). Here,

$$\overline{\mathbb{M}}_i^{\mathrm{T}(\pm)}(\mathbf{q}, \mathbf{k}) = \frac{J_1}{\hbar\omega_0}\left(\frac{\hbar}{nNM}\right)^{\frac{1}{2}}\frac{1}{2}\left(\mathbb{A}_i^{\pm} + \mathbb{D}_i^{\pm}\right)\frac{1}{\sqrt{\omega_i(\mathbf{q})}} \tag{13}$$

where $J_1/J_0 \sim 2$ Å^{-1} in graphene and the second term in parenthesis takes non-zero values for $i \neq 3, 6$, otherwise it should be treated as zero. For an $(n, 0)$ SWCNT, the coefficients of $\mathbb{A}_i^{\pm}$ and $\mathbb{D}_i^{\pm}$ are the functions of parameters included in the theory and are all presented as follows:

$$\begin{aligned}
\begin{pmatrix}\mathbb{A}_{1(4)}^{+(-)}\\ \mathbb{A}_{5(2)}^{+(-)}\end{pmatrix} &= \sqrt{3}\begin{pmatrix}s_z C_1^{\pm}\\ c_z C_2^{\pm}\end{pmatrix}\\
\begin{pmatrix}\mathbb{A}_{1(4)}^{-(+)}\\ \mathbb{A}_{5(2)}^{-(+)}\end{pmatrix} &= \mathrm{i}\sqrt{3}\begin{pmatrix}s_z S_1^{\pm}\\ c_z S_2^{\pm}\end{pmatrix}\\
\begin{pmatrix}\mathbb{A}_{6(3)}^{-(+)}\\ \mathbb{A}_{6(3)}^{+(-)}\end{pmatrix} &= -\begin{pmatrix}\mathrm{i}(S_1^{\pm} + S_3^{\pm})\\ (C_1^{\pm} - C_3^{\pm})\end{pmatrix}
\end{aligned} \tag{14}$$

with

$$C_1^{\pm} = \pm\left(c_{kq}^0\widetilde{c}_{\alpha\gamma} \pm c_k^0 c_\gamma\right), \qquad C_2^{\pm} = \pm\left(s_{kq}^0\widetilde{s}_{\alpha\gamma} \pm s_k^0 s_\gamma\right)$$

$$S_1^{\pm} = \mp\left(s_{kq}^0\widetilde{c}_{\alpha\gamma} \mp s_k^0 c_\gamma\right), \qquad S_2^{\pm} = \pm\left(c_{kq}^0\widetilde{s}_{\alpha\gamma} \mp c_k^0 s_\gamma\right)$$

$$C_3^{\pm} = c_{2k}^0 \pm c_{2kq}^0, \qquad S_3^{\pm} = s_{2k}^0 \mp s_{2kq}^0$$

for the nearest neighbor and

$$\begin{aligned}
\mathbb{D}_1^+/c_z = \mathbb{D}_5^+/s_z &= \widetilde{c}_\alpha c_q^0 - \widetilde{s}_\alpha s_q^0 - 1\\
&\quad + \mathrm{i}\left(s_{kq}^0\widetilde{c}_{\alpha\gamma} + c_{kq}^0\widetilde{c}_{\alpha\gamma} - s_k^0 c_\gamma - c_k^0 s_\gamma - \widetilde{c}_\alpha s_q^0 - \widetilde{s}_\alpha c_q^0\right)\\
\mathbb{D}_2^+/s_z = \mathbb{D}_4^+/c_z &= \widetilde{c}_\alpha c_q^0 - \widetilde{s}_\alpha s_q^0 + 1 + s_{kq}^0\widetilde{s}_{\alpha\gamma}\\
&\quad - c_{kq}^0\widetilde{c}_{\alpha\gamma} - c_k^0 c_\gamma + s_k^0 s_\gamma - \mathrm{i}\left(\widetilde{c}_\alpha s_q^0 + \widetilde{s}_\alpha c_q^0\right)\\
\mathbb{D}_1^-/c_z = \mathbb{D}_5^-/s_z &= c_{kq}^0\widetilde{c}_{\alpha\gamma} - s_{kq}^0\widetilde{s}_{\alpha\gamma} - \mathrm{i}\left(c_\gamma s_k^0 + s_\gamma c_k^0\right)\\
\mathbb{D}_2^-/s_z = \mathbb{D}_4^-/c_z &= -\mathrm{i}\left(s_{kq}^0\widetilde{c}_{\alpha\gamma} + c_{kq}^0\widetilde{s}_{\alpha\gamma}\right) - \left(c_\gamma c_k^0 - s_\gamma s_k^0\right)
\end{aligned} \tag{15}$$

for bond bending interactions.

To test our theory further, in figure 3, for a $(10, 0)$ zigzag SWCNT, we compare the analytical results of equation (11) with numerical ones in [22]. Our theory agrees in some respects with the work of Jeon and Mahan [22]. Both theories give six non-degenerate modes, of which two are acoustical and the rest are optical for $\alpha = 0$. One of two acoustical modes, $\widetilde{\omega}_3$ is longitudinal and arises from the quantization of Q_z component, and the other is a torsional one and arises from the Q_θ component; they have velocities near the Γ-point, $\upsilon_3 = 22.35$ km s^{-1} and $\upsilon_2 = 12.74$ km s^{-1}, respectively. The higher two optical modes $\widetilde{\omega}_5$ and $\widetilde{\omega}_6$, which arise from q_θ and q_z, are 1580.30 cm^{-1} and 1600 cm^{-1}, respectively, and Raman active. The remaining two optical modes $\widetilde{\omega}_1$ and $\widetilde{\omega}_4$ take place at 326.76 cm^{-1} and 877.13 cm^{-1} at the Γ-point, and arise from Q_ρ and q_ρ, respectively. Moreover, when moving away from the Γ-point towards the boundary of the Brillouin zone, two higher optical modes mix with each other. In other respects, there are some deviations; in particular, (i) the lower optical mode $\widetilde{\omega}_1$ crosses two acoustical modes; (ii) our results do not show upward curvature of the highest LO-phonon dispersion, i.e. overbending feature; (iii) the inset of figure 4 shows that equation (11) for $\alpha = \mp 2$ overestimates the lowest LO-phonon

mode; (iv) the appearance of a flexure mode for $\alpha = \mp 1$ differs from those obtained in our work.

The overall behavior of calculated results from equation (12) is shown in figure 4. In this figure, drawing the phonon dispersion curves so as to span the whole range of α variation, we get a three-dimensional picture, i.e. ω as a function of both qc and α. We note that α quantum numbers increase as the radius R of the tube increase. This means exactly that, for very large R, α becomes continuous, so that the shown projectiles create phonon dispersions along the circumferential direction, which corresponds to the $\Gamma K'$ direction of the graphene [36]. For tubes with large radius, such a picture helps us to visualize the two-dimensional **k**-vector dependence of the energy surfaces of the graphene.

In summary, our theory outlined above presents explicit analytical expressions for all phonon modes in zigzag SWCNTs and associated electron–phonon interaction amplitudes. As also emphasized earlier, the origin of the discrepancies with the existing literature may be due to the non-inclusion of bilinear terms in phonon creation and annihilation operators. The diagonalization of such terms should be further investigated.

Acknowledgments

The authors would like to thank cordially Professor T Altanhan for many continuing enlightening discussions and comments.

Appendix

All the non-zero matrix elements $\mathbb{A}_{ij}^{(k)}$ of the square matrix $\mathbb{A}$ of order 6×6 can be calculated directly from $\chi_{\mathbf{q},j}^{(i)k} = \delta_i^k \cdot (\mathbf{Q}_k^{(i)} - \mathbf{Q}_\mathrm{A})$ such that the diagonal ones are

$$\begin{aligned}
\mathbb{A}_{11}^{(1)} &= \mathbb{A}_{44}^{(1)} = 3\,(s_z)^2/2 \\
\mathbb{A}_{22}^{(1)} &= \mathbb{A}_{55}^{(1)} = 3\,(c_z)^2/2 \\
\mathbb{A}_{33}^{(1)} &= \mathbb{A}_{66}^{(1)} = 3/2
\end{aligned} \tag{A.1}$$

and non-diagonal ones are

$$\begin{aligned}
\mathbb{A}_{13}^{(1)} &= -\mathbb{A}_{46}^{(1)} = -\sqrt{3}s_z/2 \\
\mathbb{A}_{14}^{(1)} &= 3\left(\mathrm{e}^{\mathrm{i}\phi_1^0} + \mathrm{e}^{\mathrm{i}\phi_2^0}\right)(s_z)^2/4 \\
\mathbb{A}_{15}^{(1)} &= -\mathbb{A}_{24}^{(1)} = 3\left(\mathrm{e}^{\mathrm{i}\phi_1^0} - \mathrm{e}^{\mathrm{i}\phi_2^0}\right)s_z c_z/4 \\
\mathbb{A}_{16}^{(1)} &= -\mathbb{A}_{34}^{(1)} = \sqrt{3}\left(\mathrm{e}^{\mathrm{i}\phi_1^0} + \mathrm{e}^{\mathrm{i}\phi_2^0}\right)s_z/4 \\
\mathbb{A}_{25}^{(1)} &= -3\left(\mathrm{e}^{\mathrm{i}\phi_1^0} + \mathrm{e}^{\mathrm{i}\phi_2^0}\right)(c_z)^2/4 \\
\mathbb{A}_{26}^{(1)} &= \mathbb{A}_{35}^{(1)} = \sqrt{3}\left(\mathrm{e}^{\mathrm{i}\phi_1^0} - \mathrm{e}^{\mathrm{i}\phi_2^0}\right)c_z/4 \\
\mathbb{A}_{36}^{(1)} &= -\left(\mathrm{e}^{\mathrm{i}\phi_1^0} + \mathrm{e}^{\mathrm{i}\phi_2^0} + 4\mathrm{e}^{\mathrm{i}\phi_3^0}\right)/4
\end{aligned} \tag{A.2}$$

for the nearest neighbor interactions. For the next nearest neighbor and bond bending interactions, they are found to be

$$\begin{aligned}
\mathbb{A}_{11}^{(2)} &= \mathbb{A}_{44}^{(2)} = 2\left[4\,(\widetilde{s}_z)^2\,C_1^2 + (s_z)^2\left(C_2^2 + C_3^2\right)\right] \\
\mathbb{A}_{22}^{(2)} &= \mathbb{A}_{55}^{(2)} = 2\left[4\,(\widetilde{c}_z)^2\,S_1^2 + (c_z)^2\left(S_2^2 + S_3^2\right)\right] \\
\mathbb{A}_{33}^{(2)} &= \mathbb{A}_{66}^{(2)} = 6\left(S_2^2 + S_3^2\right) \\
\mathbb{A}_{12}^{(2)} &= \mathbb{A}_{45}^{(2)} = 2i\,\left[4\widetilde{s}_z\widetilde{c}_z S_1 C_1 + s_z c_z\,(S_2 C_2 - S_3 C_3)\right] \\
\mathbb{A}_{13}^{(2)} &= \mathbb{A}_{46}^{(2)} = 2i\sqrt{3}s_z\,(S_2 C_2 + S_3 C_3) \\
\mathbb{A}_{23}^{(2)} &= \mathbb{A}_{56}^{(2)} = 2\sqrt{3}c_z\left(S_2^2 - S_3^2\right)
\end{aligned} \tag{A.3}$$

and

$$\begin{aligned}
\mathbb{A}_{11}^{(3)} &= \mathbb{A}_{44}^{(3)} = 2 + 4c_z\,(\widetilde{c}_\alpha \cos qc + 1) + 4c_z^2\left(\widetilde{c}_\alpha^2 + 1\right) \\
\mathbb{A}_{22}^{(3)} &= \mathbb{A}_{55}^{(3)} = 4s_z^2\widetilde{s}_\alpha^2 \\
\mathbb{A}_{14}^{(3)} &= -2\,(1 + 2c_z)\left[\mathrm{e}^{\mathrm{i}\phi_3^0} + 2\widetilde{c}_\alpha c_z \mathrm{e}^{-\mathrm{i}\phi_3^0/2}\right] \\
\mathbb{A}_{15}^{(3)} &= -\mathbb{A}_{24}^{(3)} = 2\mathrm{i}s_z\widetilde{s}_\alpha \mathrm{e}^{-\mathrm{i}\phi_3^0/2}\,(1 + 2c_z) \\
\mathbb{A}_{12}^{(3)} &= -2\mathrm{i}s_z\widetilde{s}_\alpha\left(\mathrm{e}^{-\mathrm{i}qc} + 2\widetilde{c}_\alpha c_z\right) \\
\mathbb{A}_{45}^{(3)} &= -2\mathrm{i}s_z\widetilde{s}_\alpha\left(\mathrm{e}^{+\mathrm{i}qc} + 2\widetilde{c}_\alpha c_z\right)
\end{aligned} \tag{A.4}$$

respectively. Here, we defined the phase factors for the nearest neighbor interactions as $\phi_1^0 = (qa + \alpha\theta_z)/2$, $\phi_2^0 = (qa - \alpha\theta_z)/2$ and $\phi_3^0 = -qa$, and $\phi_1 = -\phi_4 = \alpha\theta_z$, $\phi_2 = -\phi_5 = qc + (\alpha\theta_z/2)$, $\phi_3 = -\phi_6 = qc - (\alpha\theta_z/2)$ for next six nearest neighbor atoms of A. To simplify the notation we have introduced the following designations: $s_z = \sin(\theta_z/4)c_z = \cos(\theta_z/4)$, $\widetilde{s}_z = \sin(\theta_z/2)\widetilde{c}_z = \cos(\theta_z/2)$ and $S_j = \sin(\phi_j/2)C_j = \cos(\phi_j/2)$ for $j = 1, 2, \ldots, 6$.

References

[1] Kandemir B S and Altanhan T 2008 *Phys. Rev.* B **77** 045426
[2] Iijima S 1991 *Nature* **354** 56
[3] Iijima S and Ichihashi T 1993 *Nature* **363** 603
[4] Bethune D S, Klang C H, de Vries M S, Gorman G, Savoy R, Vazquez J and Beyers R 1993 *Nature* **363** 605
[5] Rao A M, Richter E, Bandow S, Chase B, Eklund P C, Williams K A, Fang S, Subbaswamy K R, Menon M, Thess A, Smalley R E, Dresselhaus G and Dresselhaus M S 1997 *Science* **275** 187
[6] Journet C, Maser W K, Bernier P, Loiseau A, Lamy de la Chapelle M, Lefrant S, Deniard P, Lee R and Fischer J E 1997 *Nature* **388** 756
[7] Saito R, Dresselhauss G and Dresselhaus M S 1998 *Physical Properties of Carbon Nanotubes* (London: Imperial College Press)
[8] Damnjanović M, Milošević I, Dobardžić E, Vuković T and Nikolić B 2005 *Applied Physics of Carbon Nanotubes* ed S V Rotkin and S Subramoney (Berlin: Springer) pp 41–85
[9] Charlier J-C, Blase X and Roche S 2007 *Rev. Mod. Phys.* **79** 677
[10] Tang Z K, Zhang L, Wang N, Zhang X X, Wen G H, Li G D, Wang J N, Chan C T and Sheng P 2001 *Science* **292** 2462
[11] Kociak M, Kasumov A Yu, Guéron S, Reulet B, Khodos I I, Gorbatov Yu B, Volkov V T, Vaccarini L and Bouchiat H 2001 *Phys. Rev. Lett.* **86** 2416

[12] Iyakutti K, Bodapati A, Peng X, Keblinski P and Nayak S K 2006 *Phys. Rev.* B **73** 035413
[13] Jishi R A, Venkataraman L, Dresselhaus M S and Dresselhaus G 1993 *Chem. Phys. Lett.* **209** 77
[14] Dresselhaus M S and Eklund P C 2000 *Adv. Phys.* **49** 705
[15] Mahan G D 2002 *Phys. Rev.* B **65** 235402
[16] Popov V N, Van Doren V E and Balkanski M 2000 *Phys. Rev.* B **61** 3078
[17] Suzuura H and Ando T 2002 *Phys. Rev.* B **65** 235412
[18] Cao J X, Yan X H, Xiao Y, Tang Y and Ding J W 2003 *Phys. Rev.* B **67** 045413
[19] Ye L-H, Liu B-G, Wang D-S and Han R 2004 *Phys. Rev.* B **69** 235409
[20] Sánchez-Portal D, Artacho E, Soler J M, Rubio A and Ordejón P 1999 *Phys. Rev.* B **59** 12 678
[21] Mahan G D and Jeon G S 2004 *Phys. Rev.* B **70** 075405
[22] Jeon G S and Mahan G D 2005 *Phys. Rev.* B **72** 155415
[23] Gartstein Yu N 2004 *Phys. Lett.* A **327** 83
[24] Jishi R A, Dresselhaus M S and Dresselhaus G 1993 *Phys. Rev.* B **48** 11 385
[25] Woods L M and Mahan G D 2000 *Phys. Rev.* B **61** 10 651
[26] Lazzeri M, Piscanec S, Mauri F, Ferrari A C and Robertson J 2006 *Phys. Rev.* B **73** 155426
[27] Mahan G D 2003 *Phys. Rev.* B **68** 125409
[28] Jiang J, Saito R, Samsonidze Ge G, Chou S G, Jorio A, Dresselhaus G and Dresselhaus M S 2005 *Phys. Rev.* B **72** 235408
[29] Popov V N, Henrard L and Lambin P 2005 *Phys. Rev.* B **72** 035436
[30] Popov V N and Lambin P 2006 *Phys. Rev.* B **74** 075415
[31] Gunlycke D, Lawler H M and White C T 2008 *Phys. Rev.* B **77** 014303
[32] Damnjanović M and Vujičić M 1982 *Phys. Rev.* B **25** 6987
[33] Milošević I, Živanović R and Damnjanović M 1997 *Polymer* **38** 4445
[34] White C T, Robertson D H and Mintmire J W 1993 *Phys. Rev.* B **47** 5485
[35] White C T and Todorov T N 1998 *Nature* **323** 240
[36] Ando T 2005 *J. Phys. Soc. Japan* **74** 777